Electronic Supplementary Material (ESI) for Green Chemistry.

Towards feasible and scalable solvent-free enzymatic polycondensations: integrating robust biocatalysts with thin film reactions

Electronic Supplementary Information

1. Recyclability of the covalently immobilized CaLB

The course of the reaction was monitored by exploiting the ^{1}H-NMR signal at δ=1.26 of the methyl group ($C\underline{H}_3$-CH_2-O) and the signal at δ=2.33 (-CH_2-$C\underline{H}_2$-C(O)O-), the latter assumed constant throughout the reaction. Conversions were evaluated at 10, 20, 40 and 300 minutes over 8 recycles.

^{1}H-NMR (600 MHz, $CDCl_3$): δ 1.26, t, 3H, $C\underline{H}_3$-CH_2-O-; 1.48 t, 2H, -$C\underline{H}_2$-CH_2-OH; 1.56 t, 2H, -$C\underline{H}_2$-CH_2-OC(O); 1.68 t, 2H, -$C\underline{H}_2$-CH_2-C(O)O-; 2.33 t, 2H, -CH_2-$C\underline{H}_2$-C(O)O-; 3.53 t, 2H, -CH_2-$C\underline{H}_2$-OH; 4.08 t, 2H, -$C\underline{H}_2$OC(O); 4.23 CH_3-$C\underline{H}_2$-O- .

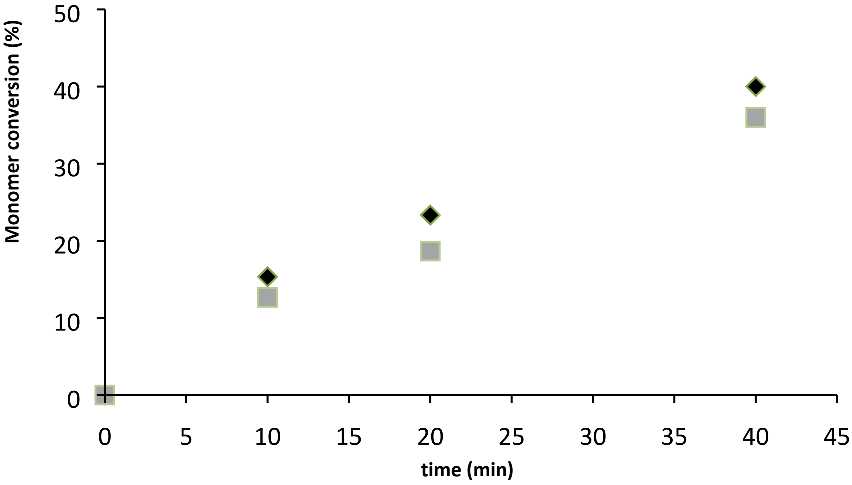

a.

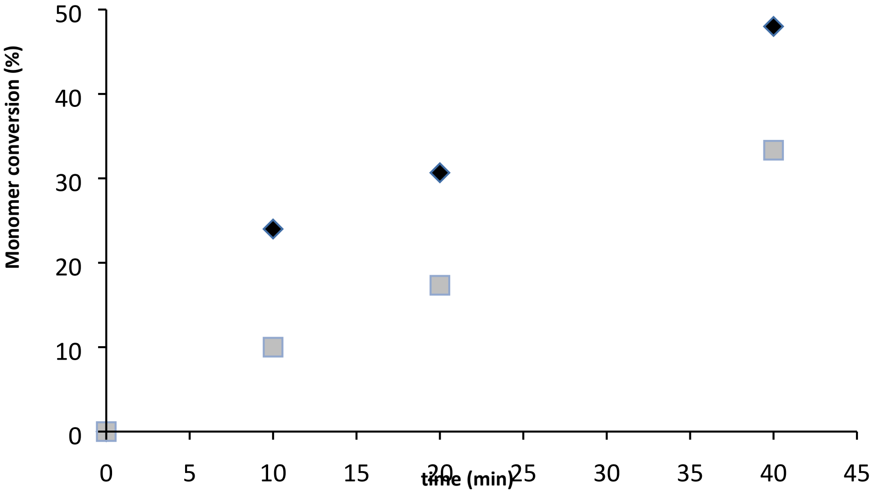

b.

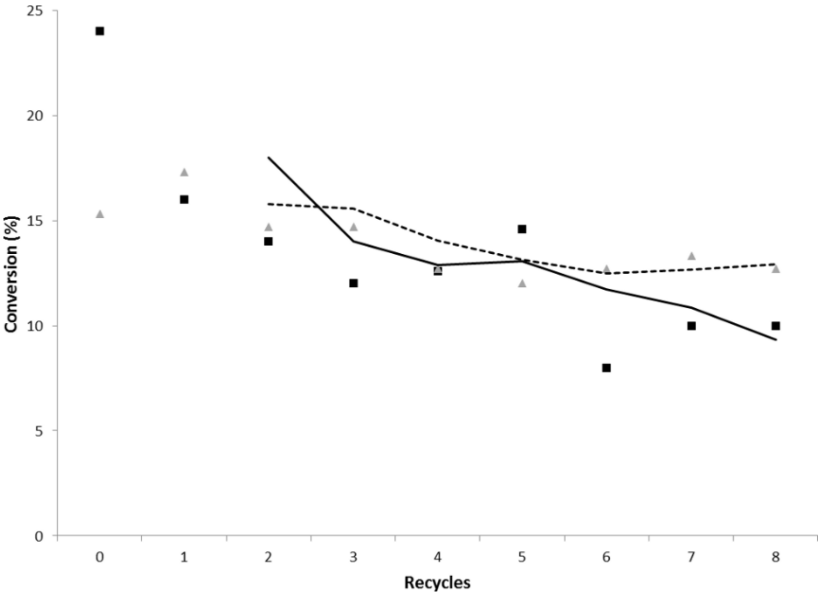

c.

Figure S1. Monomer conversion (extrapolated from ^{1}H-NMR) obtained using CaLB-Cov (a) and Novozym® 435 (b) and evaluated at different reaction times during the first synthetic cycle (black diamonds) and during the 8th cycle (gray squares).
c: Weighted moving average of conversions at 10 min measured after each cycle. Dashed line-triangles: CaLB-Cov. Black line-squares: Novozym® 435. The plot illustrates how Novozym® 435 undergoes a initial severe decrease of activity. Then the biocatalyst undergoes a continuous progressive reduction of activity as well as a wider fluctuation of the observed conversions as compared to CaLB-Cov. That behavior is ascribable to the uncontrolled release of the free enzyme so that the progress of the reaction depends on both the immobilized and free lipase.

Table S1. Solvents tested for their ability to dissolve the reaction mixture and considered as possible candidates for rinsing the biocatalysts during the recycling study. DMSO, 1,4-dioxan and THF resulted able to dissolve both reactants and products but caused a severe reduction of the hydrolytic activity (>50%). The biocatalysts were washed on the filter and under reduced pressure three times with 5 mL of solvent. Then the biocatalyst was rinsed with 10 mL of acetone to remove traces of solvent and dried over the filter before assaying the hydrolytic activity.

Solvent	**Monomer mixture**	**Reaction mixture**
THF	soluble	soluble
Acetone	soluble	partially soluble
DMSO	soluble	soluble
1,4-Dioxan	soluble	soluble
DCM	NOT soluble	soluble
Methanol	n.a.	NOT soluble
Diethyl ether	n.a.	NOT soluble

n.a.: data not available

2. Integrity of the immobilized biocatalyst after polycondensation on thin film

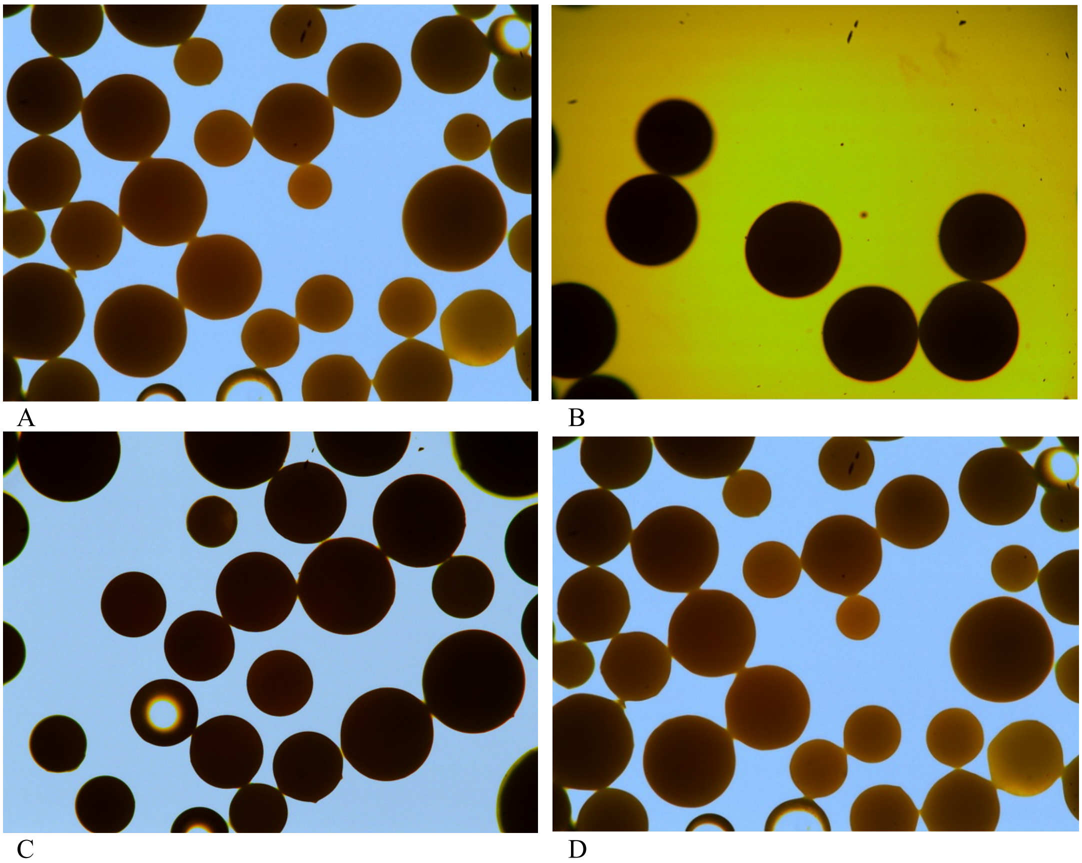

Figure S2. Samples of the covalently immobilized biocatalyst (100 x enlargement, microscope METTLER FP52). Samples A and B: biocatalyst before the synthetic process. Samples C and D: biocatalyst as recovered at the end of 3 cycles of conversion carried out according to the protocol described for the polycondensation of DEA and BDO on 10 g scale, in a round bottom flask connected to a rotary evaporator operated at 200 rpm and at 70 mbar.

3. Polycondensation of DMI and BDO

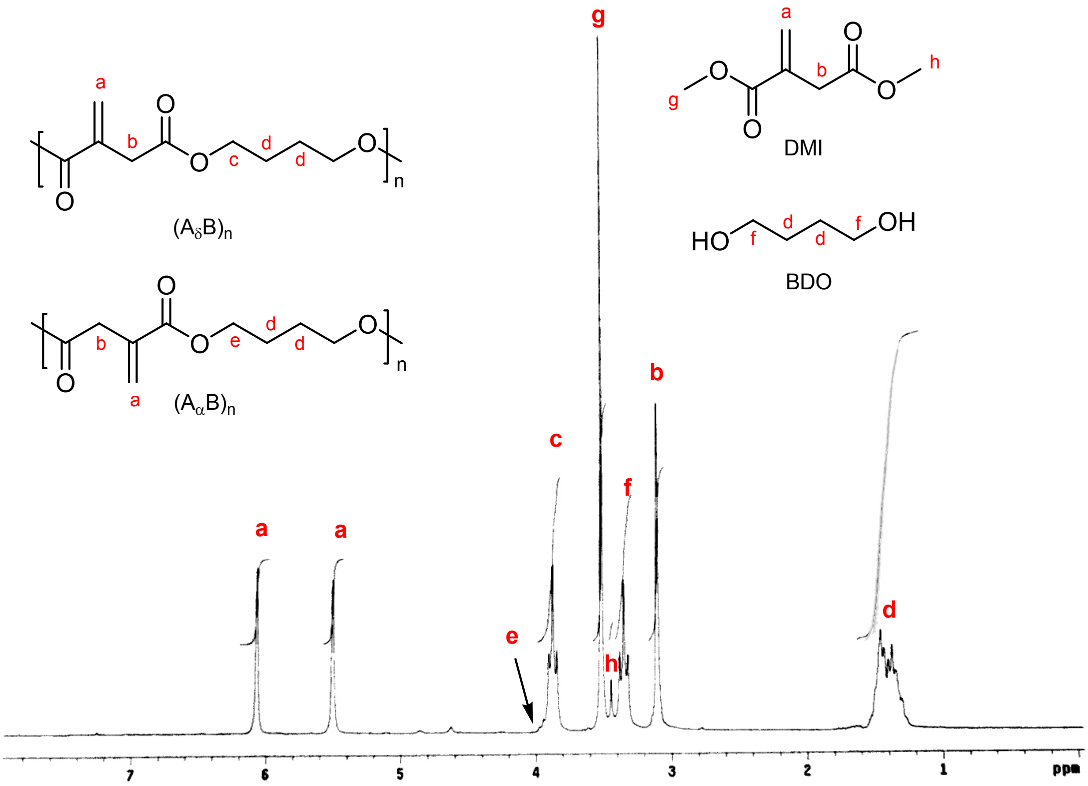

Figure S3. Fully labeled ^{1}H-NMR spectrum of polycondensation product of DMI with BDO catalyzed by CaLB-Cov in $CDCl_3$. Reaction time: 72 hours.

The signals corresponding to the preserved pendant alkene of the itaconate group can be easily distinguished at 5.6 and 6.2 ppm (a). The methylene from the itaconate structure produces a singlet at ~ 3.3 ppm (b). The methoxy groups of unreacted DMI give signals at ~ 3.57 ppm (h) and 3.64 ppm (g), respectively.

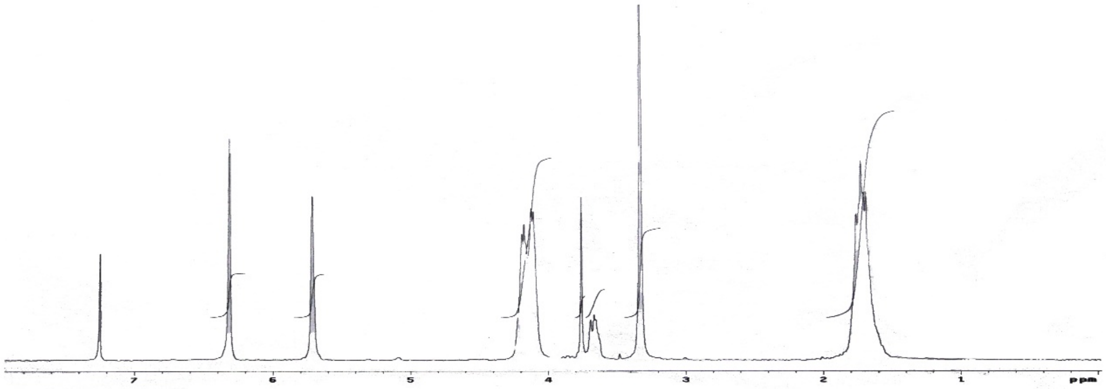

Figure S4. ^{1}H-NMR spectrum of PBI obtained from the polycondensation catalyzed by Novozym® 435. Reaction time: 96 h. ^{1}H-NMR ($CDCl_3$), δ: 1.65 (-C$\underline{H}_2$-CH$_2$-OH), 3.22 ((=C -C$\underline{H}_2$-CO), 3.57 (-CH$_2$-C$\underline{H}_2$-OH), 3.68 (C=C-CO-OC$\underline{H}_3$), 4.19 (-C$\underline{H}_2$-OCO-), 5.65 (-CO- C=C$\underline{H}$H-), 6.27 (-CO-C=CH$\underline{H}$-).

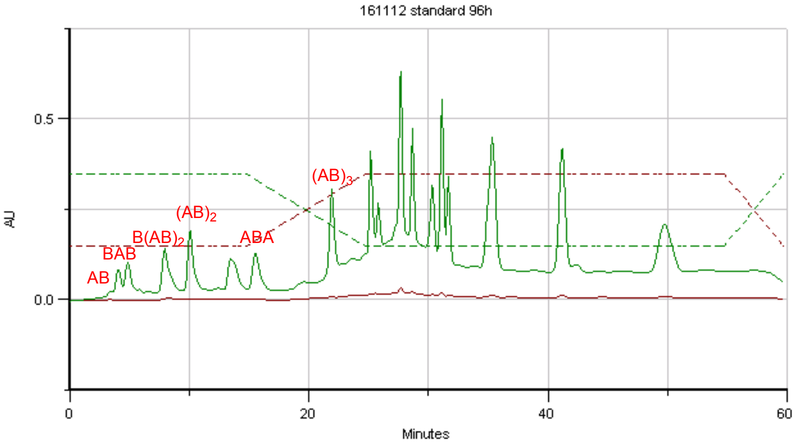

Figure S5. HPLC-DAD chromatogram of polycondensation product (PBI) of DMI with BDO catalyzed by Novozym® 435. Reaction time: 96 hours.

4. Evaluation of accessibility of the active site of covalently immobilized CaLB

4.1 Elongation catalyzed by CaLB-Cov using a PBI oligomeric mixture and DMA

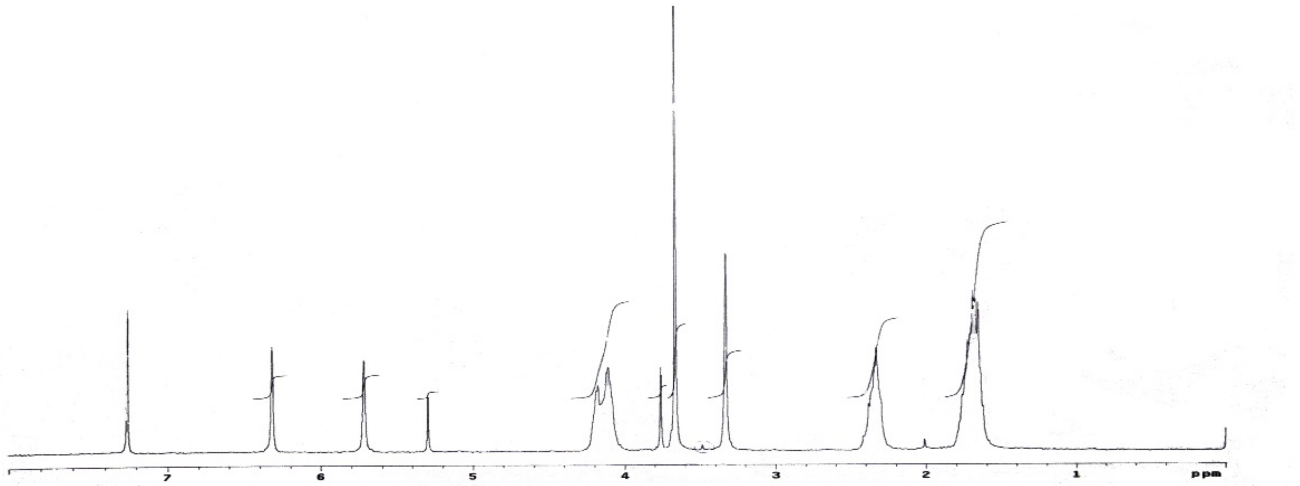

Figure S6. ^{1}H-NMR spectrum of the polycondensation product PBIA catalyzed by CaLB-Cov (elongation step). Reaction time: 72 hours. ^{1}H-NMR ($CDCl_3$), δ: 1.58-1.65 ($CH_2\text{-}C\underline{H}_2\text{-}CH_2$.CO and $\text{-}C\underline{H}_2\text{-}CH_2\text{-}OH$), 2.24 (2H, t, $\text{-}CH_2\text{-}C\underline{H}_2\text{-}CO\text{-}$), 3.22 ($=CC\underline{H}_2\text{-}COO$), 3.66 ($CH_2\text{-}COOC\underline{H}_3$), 3.69 ($C=C\text{-}COOC\underline{H}_3$), 4.19 ($\text{-}C\underline{H}_2\text{-}OCO\text{-}$), 5.65 ($\text{-}CO\text{-}C=C\underline{H}H\text{-}$), 6.27 ($\text{-}CO\text{-}C=CH\underline{H}\text{-}$).

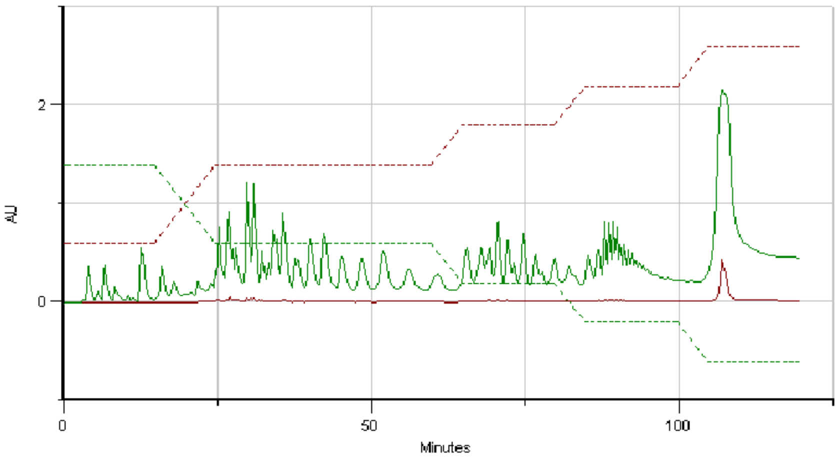

Figure S7. HPLC-DAD chromatogram of polycondensation products of PBI and DMA catalyzed by CaLB-Cov. Reaction time: 72 hours.

4.2 Hydrolysis of PBI catalyzed by CaLB-Cov

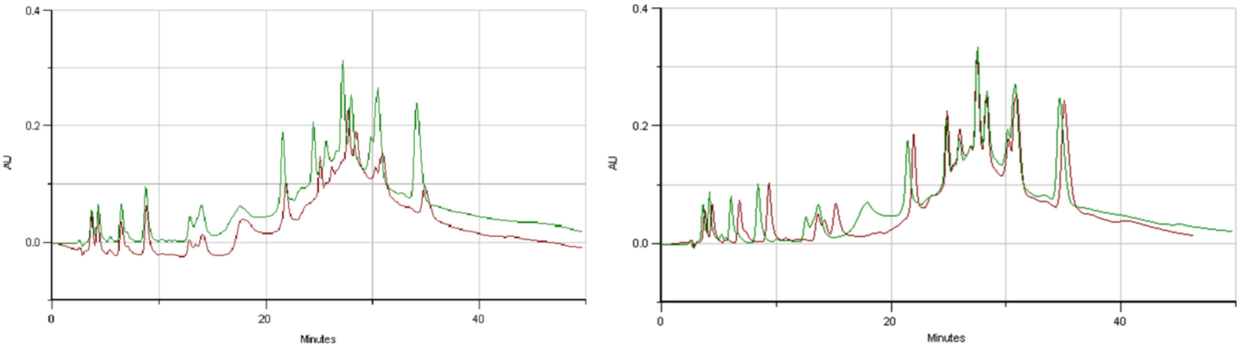

Figure S8. Left: HPLC-DAD chromatogram of hydrolysis product of PBI catalyzed by CaLB-Cov. Green: Time= 0; Red: reaction time 5 hours. Right: HPLC-DAD chromatogram of control reaction without enzyme. Green: reaction time 0 hours; Red: reaction time 5 hours.

5. HPLC-DAD analysis of the polycondensation products

Table S2. HPLC gradient used for the analysis of PBI.

Time (min)	H_2O (% vol)	AcN (% vol)
0	40	60
15	40	60
25	60	40
55	60	40
60	40	60
65	40	60

Table S3. HPLC gradient used for the analysis of PBIA.

Time (min)	H_2O (% vol)	AcN (% vol)
0	40	60
15	40	60
25	60	40
60	60	40
65	70	30
80	70	30
85	80	20
100	80	20
105	90	10
120	90	10

6. Monitoring the two-step polyesterification of AA and BDO via NMR

The progress of the reaction during each step was monitored by calculating the ratio between ^{1}H signals at δ 3.53 (t, 2H, $-CH_2-C\underline{H}_2-OH$) and at δ 4.08 (t, 2H, $-C\underline{H}_2OC(O)$).

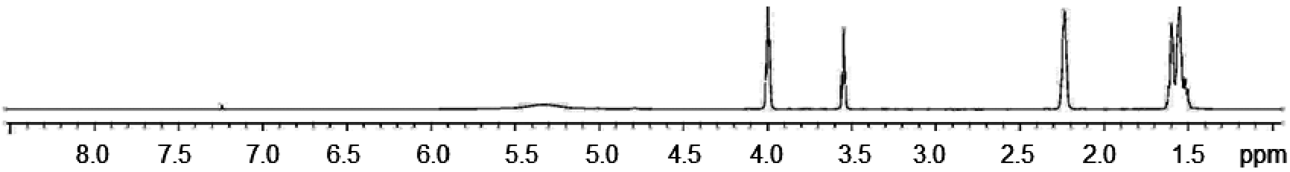

Figure S9. ^{1}H-NMR of products obtained after first step of polycondensation of AA and BDO at atmospheric pressure. ^{1}H-NMR (600 MHz, $CDCl_3$): δ 1.48 t, 2H, $-C\underline{H}_2-CH_2-OH$; δ 1.56 t, 2H, $-C\underline{H}_2-CH_2-OC(O)$; δ 1.68 t, 2H, $-C\underline{H}_2-CH_2-C(O)O-$; δ 2.25 t, 2H, $-CH_2-C\underline{H}_2-C(O)O-$; δ 3.53 t, 2H, $-CH_2-C\underline{H}_2-OH$; δ 4.08 t, 2H, $-C\underline{H}_2OC(O)$.

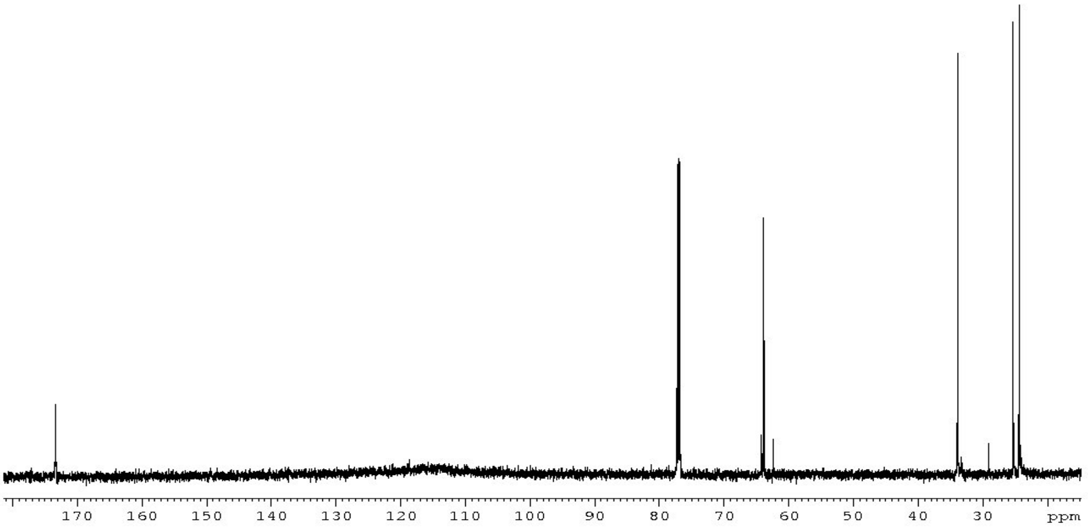

Figure S10. ^{13}C NMR of products of polycondensation of AA and BDO (600 MHz, $CDCl_3$):) δ: 24.3, $-\underline{C}H_2-CH_2-C(O)O-$; 25.1 $-\underline{C}H_2-CH_2-CH_2-OH$; 25.3 $-\underline{C}H_2-CH_2-OC(O)$; δ 29.1 $-CH_2-\underline{C}H_2-CH_2-OH$; 33.9 $-\underline{C}H_2C(O)O$; 62.6 $-CH_2-\underline{C}H_2-OH$; 63.9 $-CH_2-\underline{C}H_2-OC(O)$; 64.1 $\underline{C}H_2-CH_2-CH_2-CH_2-OH$; 173 $-CH_2O\underline{C}(O)$.

The correct assignment of signals of polymerization products was performed by 2D-^{1}H-TOCSY-^{13}C-HSQC.

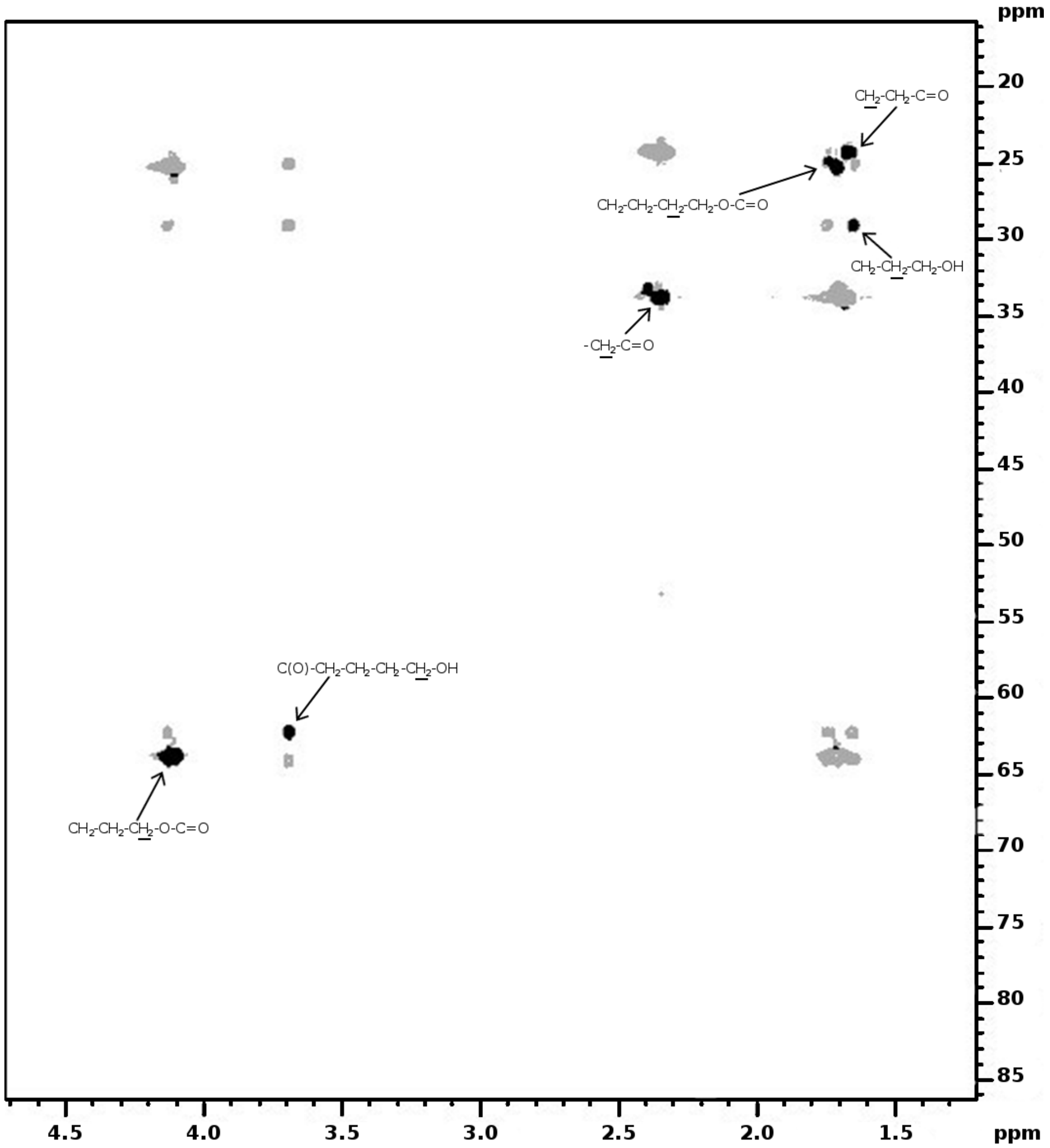

Figure S11. 2D-^{1}H-TOCSY-^{13}C-HSQC of the polymer obtained from AA and BDO following the two steps polycondensation procedure.

The spectra evidences that BDO is correlated with AA demonstrating that the reaction is completed. Once the signals were correctly assigned, it was possible to monitor the reaction progress (for both steps) by measuring the ratio between signals at δ 3.53 (t, 2H, $-CH_2-C\underline{H}_2-OH$) and at δ 4.08 (t, 2H, $-C\underline{H}_2OC(O)$).

List of abbreviations

AA	Adipic acid
AcN	Acetonitrile
BDO	1,4-butanediol
CaLB	*Candida antarctica* lipase B
CaLB-Cov	Covalently immobilized *Candida antarctica* lipase B on methacrylamide polymer
$CDCl_3$	Deuterated chloroform
DCM	Dichloromethane
DEA	Diethyl adipate
DMA	Dimethyl adipate
DMI	Dimethyl itaconate
ESI-MS	Electron Spray Ionization-Mass
HPLC-DAD	High Performance Liquid Chromatography-Diode Array Detector
IA	Itaconic acid
M_n	Number average molecular weight
PBI	poly(1,4-butylene itaconate)
NMR	Nuclear Magnetic Resonance
PBIA	poly(1,4-butylene itaconate-*co*-adipate
PDI	poly(1,4-butylene adipate)
TBU	Tributyrin hydrolytic Units
TOCSY-^{13}C-HSQC	Total Correlation Spectroscopy-^{13}C-Heteronuclear Single Quantum Coherence Spectroscopy